Korean J. of Chem. Eng., **11**(3), 190-197 (1994)

AN EXPERIMENTAL STUDY ON FLUID FLOW CHARACTERISTICS OF SUPERPOSED POROUS AND FLUID LAYERS

Dong Shik Kim, Eun Su Cho and Chang Kyun Choi†

Department of Chemical Engineering, Seoul National University, Seoul 151-742, Korea
(Received 10 December 1993 • accepted 31 March 1994)

Abstract—In the present study, fluid flow characteristics of a porous layer overlaid by a fluid layer were investigated through experiments. The experimental results were analyzed in comparison with theoretical results of a porous medium bounded by impermeable walls. With spheres, the slip coefficient was found to be 0.0107 for Poiseuille flow over a porous layer. As the permeability decreased, the experimental results approached the values calculated by Darcy's law and Forchheimer's equation. In addition, the effects of the presence of a fluid layer over a porous medium were examined in terms of the friction factor. The present experimental data placed in the range of the Darcy to the non-Darcy region are shown to be in reasonable agreement with the proposed correlation.

INTRODUCTION

There is an increasing interest in flow through fluid-saturated porous media because of the frequent occurrence of such a system in natural and industrial environments. A fluid flow in porous media can often be encountered in crude oil recovery processes and in underground water reservoirs. A fluid flow characteristic in these systems largely depends on physical properties and geometrical structure of a porous material and its physical information may provide a useful technique for an enhanced oil recovery and underground water utilization system. In industrial equipment, packed towers, geothermal operations, solar ponds, and nuclear repositories can be treated as porous media through which various fluids flow. In addition, a separation process using membrane as well as solidification of melted material can be included as such a system. Also the blood flow or accumulation in a pulmonary alveolar may cause instabilities that are related to the pathological conditions and an interstitial structure of lungs, and blood vessels can be idealized into porous media [1-3].

Experimental and theoretical studies on transport phenomena in porous media have been performed intensively since Darcy [4] reported Darcy's law in 1856. Since then Darcy's law has been modified by incorporating the boundary and inertial effects into Darcy's law. In 1901, Forchheimer [5] proposed an equation that can be applied to high-speed flow. An empirical equation using a hydraulic radius model was proposed by Carman [6] in 1937. For flow through a porous medium with a high permeability, Brinkman [7] argued that a frictional term must be added to Darcy's law in order to represent the momentum boundary layer adjacent to the rigid wall. In 1952, Ergun [8] proposed a correlation that expands the Carman-Kozeny's hydraulic radius theory. In 1981, Vafai and Tien [9] gave a semi-empirical equation that takes into account both the boundary layer effect and the non-Darcy effect. These equations show the deviation from Darcy's law at high velocities.

When a fluid-saturated porous medium is overlaid by a fluid layer, the transport phenomenon of one layer is influenced by that of the other layer and this interaction is affected not only by the physical properties and the structure of each layer but also by the condition of the interface between two layers. The systematic study of flow through the coupled layer of fluid and a porous medium constitutes rather a recent development in fluid mechanics. A problem with the boundary condition between different layers takes place when the Navier-Stokes equation is used for the flow in a fluid layer and Darcy's law for the flow in a porous medium. In 1967, Beavers and Joseph [10] pointed out that the no-slip boundary condition is no longer valid at the interface, and their new boundary condition is called the BJ-slip condition. The BJ-slip

†To whom all correspondences to be addressed.

condition has been justified to a certain degree [10-12].

But limited experimental data on the coupled fluid and porous layers are available since a few conditions that are necessary for analyzing the system may hardly be applied to experiments. For example, it is strictly required to alleviate the pressure difference between the upper and the lower layers in order not to cause vertical flows when horizontal parallel flows are analyzed. As Saffman [13] notified, the transition region and the precise definition of the nominal boundary are required to describe the slip velocity to higher order in precision. In theoretical calculation, the location of the nominal boundary surface will vary the slip coefficient to a large extent. In general, center line of particles of the upper top layer is taken as the nominal boundary.

Nield [14] used the BJ-slip condition for analyzing the onset of natural convection in a porous medium and criticized the danger of using the Brinkman equation with the no-slip condition. On the other hand, Vafai and Thiyagaraja [15] extended the Darcy's law with the continuity equation and no-slip condition to analyze the heat transfer mechanism in coupled porous and fluid layers.

In the present study, experimental data for various conditions are reported. Many efforts were exerted to measure an amount of flow of each channel with almost no vertical flow, and gathering more data above the Darcy regime. These data are compared with existing experimental data for packed columns and the values calculated by Darcy's law and the Forchheimer equation. In addition, a correlation which can be applied to the range from the Darcy to the non-Darcy regime, using modified Reynolds number and the friction factor, is suggested.

EXPERIMENTS

The experimental apparatus was designed similarly to that of Beavers and Joseph [10]. Most parts of the apparatus including the upstream and the downstream plenums were made of Plexiglas® and the porous medium consisted of uniform spherical glass beads which were randomly packed inside a rectangular wire mesh. Fig. 1 shows a schematic view of the apparatus. A rectangular wire mesh which was randomly packed with spherical glass beads was inserted into the channel. The size of channel was 150×8×4 cm (length, width and height, respectively) and the rectangular wire mesh used during the course of the experiments were 8 cm wide and 20 cm long. Its porous-layer height varied from 1.5 cm to 3 cm.

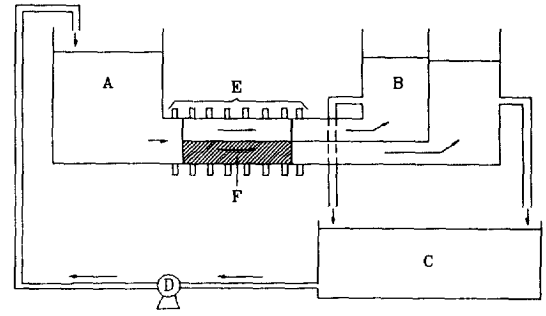

Fig. 1. Schematic of experimental apparatus.
A: Upstream plenum B: Downstream plenum
C: Reservoir D: Pump
E: Manometer taps F: Porous medium

The liquid (distilled water) levels of the upstream and downstream plenums were controlled by bypass valves for any desired height. Identical axial pressure gradients were imposed on the channel and the porous medium to give rise to parallel axial flows. Constant heads of the upstream and the downstream plenums and no pressure difference between the upper fluid layer and the lower porous medium were maintained by adjusting bypass valves of the upstream and the downstream plenum. At the downstream end of the porous medium, a sharp-edged divider plate (0.1 cm thick) set to the same height as the top of the porous layer was located and separated the efflux from the channel from that through the porous layer. The separated effluxes were guided to different plenums, respectively. The volumetric flow rate for each channel was measured separately by collecting flows from the exit of each plenum through the efflux valve for the constant time interval. The diameter of uniform particles which were used to fill in a rectangular wire was 0.45, 0.83, 2.93 and 4.93 mm each. The size of spherical particles constituting the porous medium ranged from 0.45 mm to 4.93 mm so that the permeability of the porous media ranged from 6.2×10^{-11} to 3.7×10^{-8} m^2. For example, the permeability of a porous medium was 6.2×10^{-11} m^2 for 0.45-mm particles and 3.7×10^{-8} m^2 for 4.93-mm particles.

The required head was obtained by controlling the efflux valves of the downstream plenum while maintaining a uniform liquid level in the upstream plenum. It took 5 to 30 minutes to reach a steady state of the liquid height without fluctuation. Almost no dynamic pressure difference existed between the upper fluid layer and the lower porous layer. Also, identical,

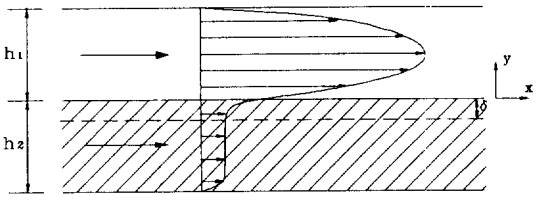

Fig. 2. Interface region between porous and fluid layers.

uniform axial pressure gradients in the channel and the porous medium were maintained. The manometers connected to pressure taps were used to check this pressure difference. Pressure taps were located along the length of the upper and the lower plates at 2 cm intervals. The pressure and flow rate were measured 5 times for each run and average values were used for the analysis.

THEORETICAL ASPECTS

1. Lower Porous Layer

The velocity profile in coupled porous and fluid layers can be represented as shown in Fig. 2. The axial and vertical coordinates are, respectively, x and y. The vertical distance y is measured from the interface between a porous layer and a fluid layer. The charateristic distance δ is used to represent the boundary layer of a porous medium and the order of magnitude of δ is the diameter of a particle d. The pressure and the velocity vary continuously in this boundary layer. An analysis of this system can be conducted by neglecting the velocity change in the boundary layer with $\delta \rightarrow 0$, in a macroscopic view. On the other hand, a rapid change of the velocity in the boundary layer can be taken into account.

Darcy's law describing flow characteristics in a porous medium is given by

$$\overline{V} = -\frac{K}{\mu}\frac{dP}{dx} \tag{1}$$

where, $\overline{V}$ represents the mean permeation velocity, K the permeability and μ the fluid viscosity. This macroscopic representation of Darcy's law, however, can be applied to only a few simple structure since the flow pass through the complex three-dimensional space. The semiheuristic models as capillary models and drag models [16] are being studied for a complicated porous medium. K may be obtained from the Carman-Kozeny equation based on the hydraulic radius model :

$$K = \frac{\varepsilon^3 d^2}{150(1-\varepsilon)^2} \tag{2}$$

where ε represents the porosity. Ergun [8] proposed the following empirical equation which extends the Eq. (1) with Eqs. (2) and (7) to a high speed range :

$$-\frac{dP}{dx} = 150\frac{(1-\varepsilon)^2}{\varepsilon^2}\frac{\mu\overline{V}}{d^2} + 1.75\frac{1-\varepsilon}{\varepsilon^2}\frac{\rho\overline{V}^2}{d} \tag{3}$$

Darcy's law neglects the effect of inertial forces and the flow near the wall or the interface between a fluid and a porous medium. When the fluid velocity or the porosity increases, discrepancy to Eq. (1) accumulates. Brinkman's equation is often used to explain the flow in the boundary layer. Forchheimer [5] argued that the inertial term be included and Vafai et al. [9, 15] considered both the inertial force and the boundary layer effect. The related equations are summarized as follows :

(Forchheimer's equation)

$$-\frac{dP}{dx} = \frac{\mu}{K}\overline{V} + \frac{\rho\beta}{K}\overline{V}^2 \tag{4}$$

(Brinkman's equation)

$$-\frac{dP}{dx} = \frac{\mu}{K}\overline{V} - \mu^*\frac{d^2\overline{V}}{dy^2} \tag{5}$$

(Vafai's equation)

$$-\frac{dP}{dx} = \frac{\mu}{K}\overline{V} + \frac{\rho\beta}{K}\overline{V}^2 - \frac{\mu}{\varepsilon}\frac{d^2\overline{V}}{dy^2} \tag{6}$$

where ρ represents the fluid density, β the Forchheimer coefficient and μ^* the effective viscosity. β can be written as

$$\beta = \frac{1.75d}{150(1-\varepsilon)} \tag{7}$$

With Darcy's law, the fluid velocity is assumed to be proportional to the pressure difference in a porous medium. But when the fluid velocity is so high, that is, in the non-Darcy regime, most of experimental results deviate from linearity and show proportionality to the square of the fluid velocity [17] :

$$-\frac{dP}{dx} = a\mu\overline{V} + b\beta\overline{V}^2 \tag{8}$$

where a and b are constants which depend on the characteristics of a porous medium. For very slow flow, Eq. (8) reduces to Darcy's law that the constant a must equal 1/K. Upon changing Eq. (8), we get

$$\frac{1}{\mu\bar{V}}\left(-\frac{dP}{dx}\right)=\frac{1}{K}+b\frac{\rho\bar{V}}{\mu} \tag{9}$$

When $(-dP/dx)/(\mu\bar{V})$ is plotted with $\rho\bar{V}/\mu$, the permeability K can be determined from the vertical intercept.

2. Upper Fluid Layer

The velocity profile in the upper channel obeys the Navier-Stokes equation for laminar flow:

$$\frac{dP}{dx}=\mu\frac{d^2u}{dy^2} \tag{10}$$

The boundary condition for the upper fluid channel are given by

$$u=0 \text{ at } y=h_1 \tag{11}$$

$$\frac{du}{dy}=\frac{\alpha}{\sqrt{K}}(u_s-\bar{V}) \text{ at } y=0^+ \tag{12}$$

where α is the slip coefficient. Eq. (12) is the well known B-J condition [10] and u_s is the slip velocity at the interface. The solution of Eq. (10) subject to Eqs. (11) and (12) yields the velocity profile in the upper channel as

$$u=u_s\left(1+\frac{\alpha}{\sqrt{K}}y\right)+\frac{K}{2\mu}\left(\frac{dP}{dx}\right)\left(\frac{2\alpha}{\sqrt{K}}y+\frac{1}{K}y^2\right) \tag{13}$$

The average velocity $\bar{u}$ and the slip velocity u_s are obtained from the above equations:

$$\bar{u}=-\frac{1}{12\mu}\left(\frac{dP}{dx}\right)h_1^2+\frac{u_s}{2} \tag{14}$$

$$u_s=-\frac{K}{2\mu}\left(\frac{\sigma^2+2\alpha\sigma}{1+\alpha\sigma}\right)\left(\frac{dP}{dx}\right) \tag{15}$$

where $\sigma=h_1/\sqrt{K}$.

An accurate value of α is required because it plays a vital role in analyzing a fluid flow and heat transfer between a fluid layer and a porous medium. The volumetric flow rate Q for a channel of width W and height h_1 is given by

$$Q=Wh_1\left\{\frac{1}{12\mu}\frac{\Delta P}{L}h_1^2+\frac{u_s}{2}\right\} \tag{16}$$

where L is the length of the channel. The volumetric flow rate of Poiseuille flow through a channel bounded by impermeable walls is given by

$$Q_0=\frac{Wh_1^3\Delta P}{12\mu L}F_s \tag{17}$$

where F_s denotes the shape factor. The flow through a channel bounded by solid walls can be written with

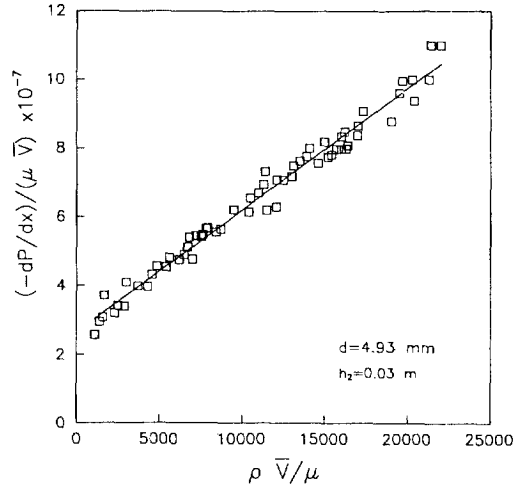

Fig. 3. Experimental data plotted as a function of $\rho V/\mu$ and $(-dP/dx)/(\mu V)$.

the flow bounded by a porous medium as

$$\frac{Q}{Q_0}=1+\frac{3(\sigma+2\alpha)}{\sigma(1+\alpha\sigma)} \tag{18}$$

This equation represents the increased portion of the volumetric flow rate due to the presence of a porous wall. Therefore, after the ratio Q/Q_0 is plotted as a function of σ, the slip coefficient α is obtained by using the least square method.

RESULTS AND DISCUSSION

1. Permeability and Slip Coefficient

One of the most important parameters in the present study is the permeability K. The permeability may be obtained by experimental data with Darcy's law, statistical models or hydraulic radius model theory. However, as the flow rate examined in the present study exceeded the Darcy regime for most cases, Darcy's law could not be simply applied. As was done by Beavers and Sparrow [18], when the present experimental results are plotted by using $\rho\bar{V}/\mu$ as the abscissa and $(-dP/dx)/(\mu\bar{V})$ as the ordinate variable, $(-dP/dx)/(\mu\bar{V})$ is observed to be a linear function of $\rho\bar{V}/\mu$ as is shown in Fig. 3. So, it is considered that the approach of Muskat [17] and Beavers and Sparrow [18] in which a porous medium is bound by four solid walls can be applied to the present porous medium, one of whose bounding walls is a fluid layer. The permeabilities calculated by this method are listed in Table 1 in terms of the particle size and the height of porous media. It is shown that the permeabi-

Table 1. Estimated K values for different d and h_2

d (mm)	h_2 (m)	K (m^2) Experimental data	Ergun equation
4.93	0.030	3.93×10^{-8}	2.40×10^{-8}
	0.020	3.70×10^{-8}	
	0.015	3.70×10^{-8}	
	0.010	3.93×10^{-8}	
2.96	0.030	1.28×10^{-10}	6.95×10^{-9}
	0.020	1.40×10^{-10}	
	0.015	1.39×10^{-10}	
	0.010	1.40×10^{-10}	
0.83	0.030	3.88×10^{-10}	3.88×10^{-10}
	0.020	3.94×10^{-10}	
	0.015	4.46×10^{-10}	
	0.010	4.43×10^{-10}	
0.45	0.030	6.24×10^{-11}	6.20×10^{-11}
	0.020	6.64×10^{-11}	
	0.015	6.72×10^{-11}	
	0.010	7.26×10^{-11}	

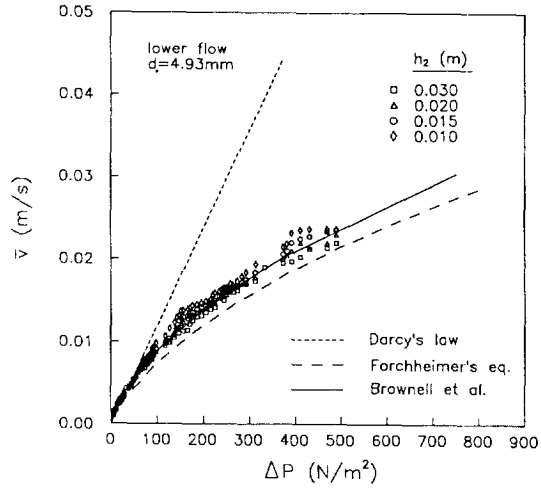

Fig. 4. Comparison of present experimental data with previous results for d=4.93 mm.

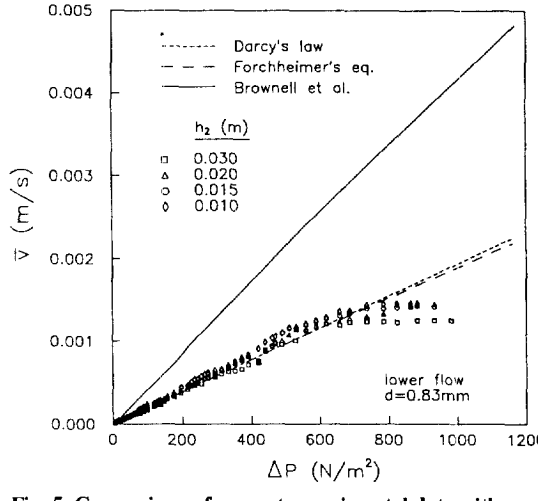

Fig. 5. Comparison of present experimental data with previous results for d=2.96 mm.

lities obtained in the present experiment are larger than those calculated from Carman-Kozeny Eq. (2) and for a constant particle size, experimental values of permeabilities increase with the height of porous media.

The Beavers-Joseph method was applied to obtain the slip coefficient α. Experimental data within the laminar regime were used so that slip coefficients could be obtained from Eq. (18). The determined values of α range from 0.0096 to 0.012. Considering the argument of Taylor [12] that α depends only on the structure of porous medium and it is almost independent on the height of the layer except a small range of the layer height (order of $K^{1/2}$), its average value 0.0107 can be taken as the slip coefficient in the present system. This value is close to that of Rajasekhara [19], who obtained 0.01 for the value of α when using sand as a porous medium.

2. Lower Porous Layer

Compared to accumulated data on fluid flow through a porous medium bounded by four solid walls, only a few experimental data on fluid flow in a porous medium overlaid by a fluid layer are available. In 1950, Brownell et al. [20] performed experiments employing a circular tube packed with various particles and presented a relationship between a modified friction factor and a modified Reynolds number. In Figs. 4 to 7 the present data are compared with their experimental data to show difference of existence of a porous bounding wall, as well as Darcy's law and Forchheimer's equation. It can be found that the fluid velocity $\bar{V}$ decreases with a decrease in particle size for a given ΔP. As the thickness of a porous layer decreased and the permeability increased, the increased slip velocity and flow velocity in an upper fluid layer affected the average velocity in a lower porous layer more strongly. With a decrease in particle size the present data followed Darcy's law, as shown in the figures. But for a lager particle system the present data were close to Brownell et al.'s.

Attention will now be directed to the presentation of the experimental data in terms of the dimensionless groups Re_b and f_b. The modified Reynolds number and

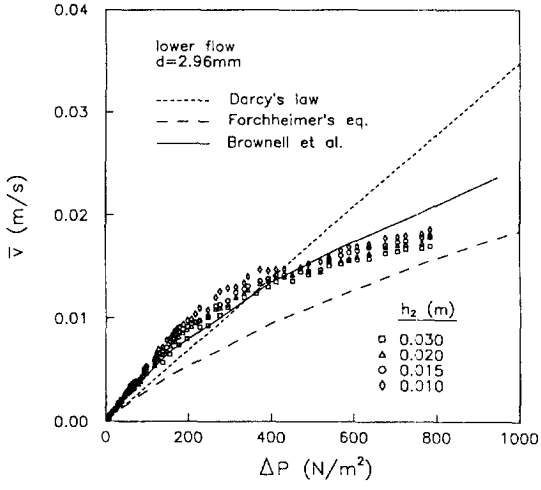

Fig. 6. Comparison of present experimental data with previous results for d=0.83 mm.

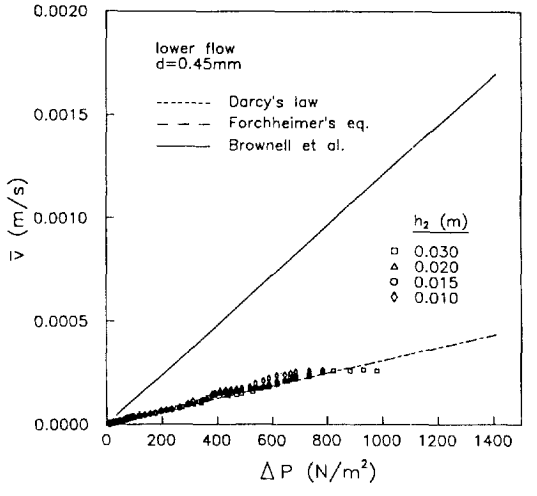

Fig. 7. Comparison of present experimental data with previous results for d=0.45 mm.

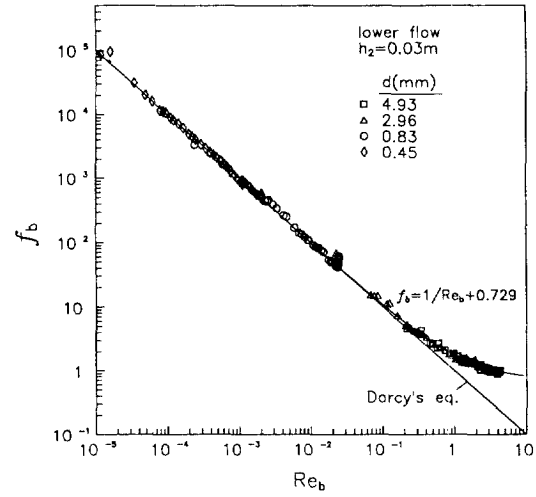

Fig. 8. Comparison of correlation (21) with experimental data for h_2=0.03 m.

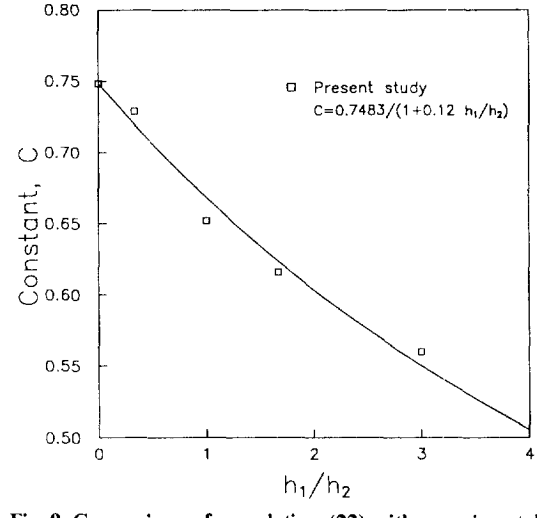

Fig. 9. Comparison of correlation (22) with experimental data.

modified friction factor by Beavers and Joseph [18] are used here and they are defined as :

$$Re_b=\frac{\rho\bar{V}\sqrt{K}}{\mu} \tag{19}$$

$$f_b=\frac{(\Delta P/L)\sqrt{K}}{\bar{V}^2\rho} \tag{20}$$

Now, by using the above relations, Eq. (9) can be transformed to

$$f_b=\frac{1}{Re_b}+C \tag{21}$$

The value of C for each set of experimental data is listed in the figures. The plot of Re_b vs. f_b for the experimental data and Darcy's equation are shown in Fig. 8. Fig. 9 shows that the C value decreases as the height of a porous medium decreases. It is assumed that the C values contain the effect of the variation of the ratio h_1/h_2 as well as the effect of the permeability change. The solid line in the figure can be correlated by

$$C=\frac{0.7483}{1+0.12\frac{h_1}{h_2}} \tag{22}$$

where h_1 represents the fluid layer thickness and h_2 porous layer thickness. Consequently the following relationship is produced :

$$f_b=\frac{1}{Re_b}+\frac{0.7483}{\left(1+0.12\frac{h_1}{h_2}\right)} \tag{23}$$

This correlation covers the present data well in the range of $Re<10$ and $0.33\leq h_1/h_2\leq 3$ with $h_1+h_2=4$ cm. Another type of correlation based on the Ergun equation was tested but data scattering became severe with an increase in particle size.

As h_1/h_2 approaches zero, which means the channel is completely filled with spheres, the constant C in the present system becomes 0.75 as a limiting case. For a fluid flow through various porous media, Eq. (21) with $C=0.55$ for particulate media was suggested by Ward [21], while $C=0.40$ for glass spheres and 0.566 for lead shot were suggested by Brownell et al. [20] and Lindquist [22], respectively. For a channel filled with metal fibers, Beavers et al. [18] proposed $C=0.074$. Therefore it is stated that C is dependent on the particulate shape and flow properties.

CONCLUSION

The factors affecting a volumetric flow rate in porous media which was overlaid by fluid layer were investigated. In the present system of spheres the B-J slip coefficient was found to have the value of 0.0107. A slight increase in volumetric flow rate in porous media due to the presence of bounding fluid layer was observed. The experimental data approached Darcy's law with a decrease in permeability and Reynolds number.

A new correlation of the friction factor was derived as a function of the Reynolds number and the ratio of the fluid layer thickness to the porous one. This correlation is in good agreement with the present experimental data.

ACKNOWLEDGEMENT

The authors wish to thank Honam Oil Refinery Co. for supporting this research.

NOMENCLATURE

d : particle diameter [m]
F_s : shape factor [-]
f_b : modified friction factor defined by Eq. (20) [-]
h_1 : fluid layer thickness [m]
h_2 : porous layer thickness [m]
K : permeability [m^2]
L : channel length [m]
P : pressure [N m^{-2}]
Q : volumetric flow rate [m^3 s^{-1}]
Re_b : modified Reynolds number defined by Eq. (19) [-]
u : channel flow velocity [m s^{-1}]
$\bar{u}$: average channel velocity [m s^{-1}]
V : velocity in porous media [m s^{-1}]
$\bar{V}$: average permeation velocity [m s^{-1}]
W : channel width [m]
x, y : positions in cartesian coordinates [m]

Greek Letters

α : slip coefficient [-]
β : Forchheimer coefficient [-]
δ : boundary layer depth [m]
ε : porosity [-]
ΔP : pressure difference [N m^{-2}]
σ : dimensionless length scale [-]
μ : fluid viscosity [kg m^{-1} s^{-1}]
μ^* : effective viscosity [kg m^{-1} s^{-1}]
ρ : density [kg m^{-3}]

Subscripts

s : slip velocity
0 : Poiseuille flow
1 : fluid layer
2 : porous layer

REFERENCES

1. Fung, Y. C. and Tang, H. T.: *J. App. Mech. Trans., ASME*, **97**, 531 (1975).
2. Fung, Y. C. and Tang, H. T.: *J. App. Mech. Trans., ASME*, **97**, 536 (1975).
3. Tang, H. T. and Fung, Y. C.: *J. App. Mech. Trans., ASME*, **97**, 45 (1975).
4. Darcy, H. P. G.: "Les Fontaines Publiques de la Ville de Digon", Vector-Dalmont, Paris (1856).
5. Forchheimer, P.: *Z. Ver. Duetsch. Ing.*, **45**, 1782 (1901).
6. Carman, P. C.: *J. Soc. Chem. Ind.*, **57**, 225 (1937).
7. Brinkman, H. C.: *App. Sci. Res.*, **A1**, 27 (1947).
8. Ergun, S.: *Chem. Eng. Prog.*, **48**, 89 (1952).
9. Vafai, K. and Tien, C. L.: *Int. J. Heat Mass Transfer*, **24**, 195 (1981).

10. Beavers, G. S. and Joseph, D. D.: *J. Fluid Mech.*, **30**, 197 (1967).
11. Beavers, G. S., Sparrow, E. M. and Magnuson, R. A.: *J. Basic Eng.*, **92**, 843 (1970).
12. Taylor, G. I.: *J. Fluid Mech.*, **49**, 319 (1971).
13. Saffman, P. G.: *Studies Appl. Math.*, **1**, 93 (1971).
14. Nield, D. A.: *J. Fluid Mech.*, **81**, 513 (1977).
15. Vafai, K. and Thiyagaraja, R.: *Int. J. Heat Mass Transfer*, **30**, 1391 (1987).
16. Kaviany, M.: "Principles of Heat Transfer in Porous Media", Springer-Verlag, N. Y., 26 (1991).
17. Muskat, M.: "The Flow of Homogeneous Fluids Through Porous Media", McGraw-Hill, N. Y. (1937).
18. Beavers, G. S. and Sparrow, E. M.: *J. App. Mech.*, **13**, 711 (1969).
19. Rajasekhara, B. M.: Ph. D. Thesis, Bangalore University, India (1974).
20. Brownell, L. E., Combrowski, H. S. and Dickey, C. A.: *Chem. Eng. Prog.*, **46**, 415 (1950).
21. Ward, J. C.: J. Hydraulics Division, Proceedings of the American Society of Civil Engineers, **90**, HY5, 1 (1964).
22. Lindquist, E. G. W.: Discussion of Refernce [21], **91**, HY3, 325 (1965).